Institute of Physics Publishing
doi:10.1088/1742-6596/32/1/011

Towards gravitational wave astronomy: Commissioning and characterization of GEO 600

S. Hild[1], H. Grote[1], J.R. Smith[1] and M. Hewitson[1] for the GEO 600-team[2]

.

[1] Max-Planck-Institut für Gravitationsphysik (Albert-Einstein-Institut) und Universität Hannover, Callinstr. 38, D–30167 Hannover, Germany.
[2] See GEO 600 status report paper for the author list of the GEO collaboration.

E-mail: `stefan.hild@aei.mpg.de`

Abstract. During the S4 LSC science run, the gravitational-wave detector GEO 600, the first large scale dual recycled interferometer, took 30 days of continuous data. An instrumental duty cycle greater than 96% and a peak sensitivity of $7 \times 10^{-22}/\sqrt{\text{Hz}}$ around 1 kHz were achieved during this time. Detector commissioning and characterization work are essential to prepare the worldwide network of gravitational-wave detectors for future extended science runs. This paper describes the detector commissioning that was done in the run-up to S4. The focus is set on techniques used for the identification and removal of limiting noise sources. Furthermore we give some examples for the detector characterization work of GEO 600.

1. Introduction

During the past few years the four large scale interferometric gravitational wave projects, LIGO [1], VIRGO [2], TAMA 300 [3] and GEO 600 [4] have dedicated much effort to commissioning the detectors and improving their sensitivity. More and more the focus of the commissioning work has shifted to preparing and settling the detectors for long data taking periods. The aim is to get a reliable and stationary detector that is as sensitive as possible and well understood and characterized.

In this paper we give an overview of detector commissioning and detector characterization work of GEO 600. In Section 2 two methods to identify limiting noise sources are described. Noise projections can deal with noise sources that couple linearly. As an example for a noise source that couples non-linearly to the main output, we explain a technique to find limiting noise introduced by stray light. Once the limiting noise is identified, naturally the highest priority is to eliminate either the noise source itself or its coupling to the detection port. In Section 3 we describe in detail the improvements we did to two control loops (Michelson differential and signal recycling loop) in order to reduce their noise contributions to the gravitational-wave sensitive detector output.

To increase the detector stability we developed a procedure to analyse losses of lock. This is presented in Section 4.1. Guaranteeing high data quality is one of the main goals of detector characterization. Nevertheless, due to imperfections of the detector sometimes poor data quality cannot be avoided. For these times data quality flags need to be defined. As an example, the

© 2006 IOP Publishing Ltd

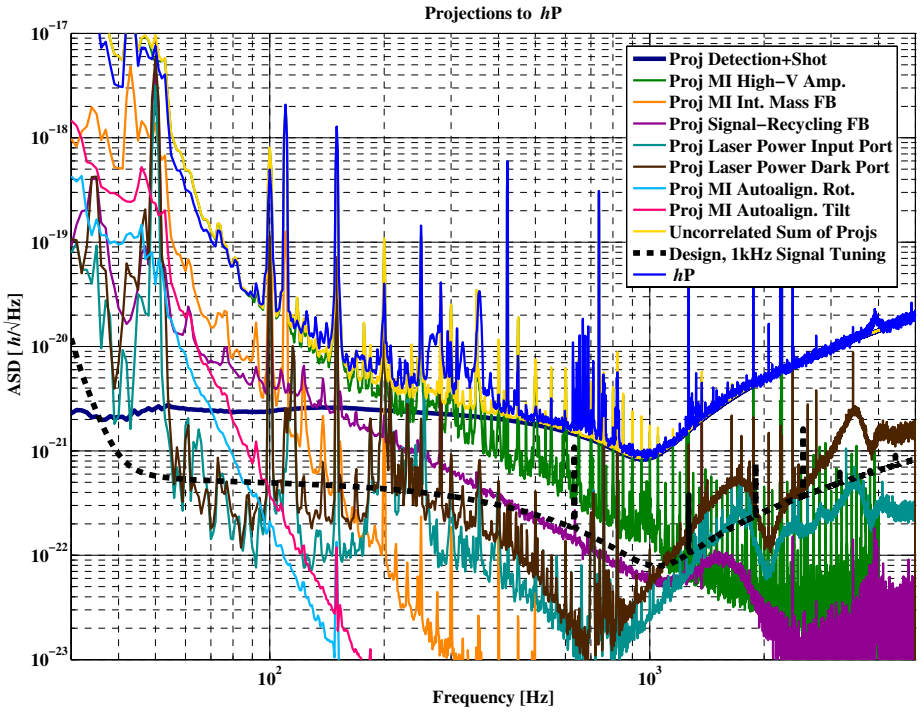

Figure 1. Noise projection of various signals for a time of the S4 LSC science run. At high frequencies the sensitivity is limited by a mixture of detection and shot noise, while below 200 Hz noise introduced by the high voltage amplifiers used for the electrostatic drives is dominating.

definition and application of the χ^2 data quality flag is shown in Section 4.2. Finally in Section 4.3 the performance of GEO 600 during the 30 days of the LSC science run S4 is described.

2. Identification of limiting noise sources

2.1. Noise projections

Many different kinds of technical noise sources couple to the detector output and can limit the detector's sensitivity. To identify which of these contribute to the actual noise in the gravitational wave signal, we use so called 'noise projections'. To project a given noise source n, which is recorded in the channel N to the detector output E, one has to measure the transfer function $T_{N\to E}$ from N to E, while injecting a signal into the path where n couples. In a second step the noise spectrum of N has to be measured and multiplied by the transfer function $T_{N\to E}$ to get the projection. With this method it is possible to project all noise sources that couple linearly.

Ideally, noise projections are performed while all control systems are at their nominal operating points. However, these measurements can be limited by loop gain problems and are practically useful only at frequencies for which the loop gain of the associated control loops is less than unity. This problem can be avoided by opening the loop and dividing it into smaller parts for which the noise projections are done separately. However the derived noise contribution only represents one moment in time. Further details of the noise projection techniques are beyond the scope of this paper and can be found in [5]. Figure 1 shows a set of noise projections for a time of S4.

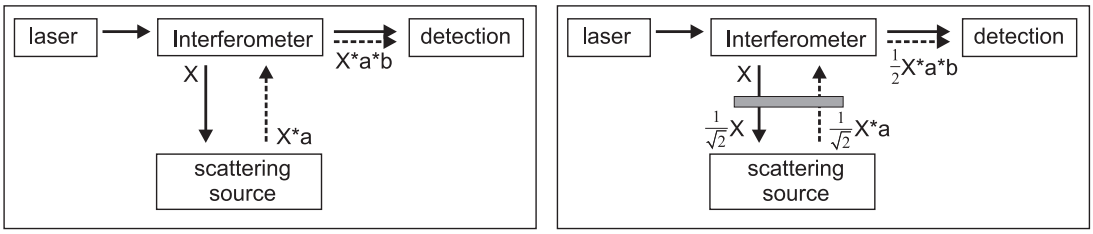

Figure 2. Sketch of the filter experiment (description is given in Section 2.3).

2.2. Non-linearly coupling noise sources

Unfortunately there is no general procedure available to identify noise sources that not necessarily couple linearly to the output, like scattered light or acoustic noise. One successful approach we found is to slightly vary the suspicious noise source or its coupling and look for correlated changes in the strain signal. Of course, this method only works if the corresponding noise already limits *h(t)* or is at least close to limiting. As an example, we will describe a method we call the 'filter experiment' which is very effective at identifying limiting scattered light sources.

2.3. The filter experiment – an easy way to identify scattered light

At the end of 2004, GEO 600 was limited by noise caused by stray light. At numerous points of an interferometric gravitational wave detector, light is coupled out of the main interferometer path to auxiliary paths that are used for control and diagnostics of the detector. If some light is scattered back into the interferometer from any component in such an auxiliary path, this light may have a varying undefined phase and can cause excess noise in the detector output. By using the filter experiment it is easy to find the origin of the scattering. A neutral density filter is placed sequentially in the auxiliary paths, which should in principle not spoil the sensitivity [1]. If X is the amount of light leaving the interferometer as an auxiliary beam and a and b are the scattering efficiency and the backcoupling coefficient into the main interferometer, respectively, then $X \times a \times b$ represents the amplitude of stray light at the detection port.

Suppose we insert an absorption filter with an attenuation of $\sqrt{2}$ in amplitude between the main interferometer and the auxiliary path. By doing this, the amplitude of the light present at the scattering source is reduced from X to $\frac{X}{\sqrt{2}}$. Due to the fact that the scattered light also gets attenuated by the filter, the scattered light that actually arrives at the detection port is halved. This corresponds to an improvement in sensitivity, provided the scattered light was dominating the noise without the filter.

Using this method, we were able to find that scattered light in an auxiliary path coming from the beamsplitter's anti-reflection coating was limiting the sensitivity for frequencies between 150 Hz and 1.2 kHz. By improving the optical setup we were able to reduce the scattering to a level such that we could no longer detect a coupling to the detector output. This resulted in an improvement of about a factor of 3 in sensitivity over most of the frequencies mentioned above.

3. Noise reduction

Once the limiting noise sources are identified, either the levels of the noises at their origins or their couplings to the detector output have to be reduced. In general we have to deal with three types of noise. First of all, feedback noise is introduced by the electronics that keep all mirrors at their required positions. Secondly, light and modulation noises occur, for example

[1] This is valid as long as reducing the signal in the auxiliary path by the power transmission factor of the filter does not cause an associated noise to limit the detector output.

due to fluctuations in light power and modulation phase. Non-linearly coupling noise sources, like acoustics, scattered light and frequency noise, form the third group. In the following two sections we will give two examples of reducing feedback noise.

3.1. Michelson longitudinal noise

As *h(t)* is derived from the Michelson differential errorpoint, all noises present in the Michelson longitudinal loop couple directly to *h(t)*. In this loop, limiting noise contributions from electronics between the photodetector and the feedback point were reduced by redistributing the electronic gain within the circuit to improve the signal-to-noise-ratio over the limiting frequency range. After this improvement in the detection path this loop was limited by actuator noise in the feedback path. To guarantee extremely low thermal noise of the test masses, GEO 600 does not use magnet-coil actuators, but electrostatic drives (ESD) in combination with a high voltage amplifier (HVA) [6].

For such an actuator the force applied to the test masses is proportional to the square of the applied voltage. In order to make the force linear, the square-root of the feedback signal is generated by a circuit before application to the actuator. The use of the square root circuits has the drawback of introducing additional electronic noise, but it is indispensable to provide the linear range needed for lock acquisition. Once the Michelson loop is locked, the necessary linear range is small enough to allow the switching off of the noisy square-root circuits. [2]

In order to use the ESD as a bipolar displacement actuator, a constant bias force has to be applied to the ESD. The linear actuator range is determined by the level of this bias. On the other hand the introduced noise level is also proportional to this bias. Again we would like to have a linear range as large as possible for lock acquisition, but we can reduce the noise by lowering the bias, after lock is established. Since the noise introduced by the nonlinearity of the ESD actuators is proportional to $1/\text{bias}^2$, we can decrease the bias only by a certain amount.

Recently we also implemented a whitening / dewhitening technique as another means of reducing electronic noise in the feedback loop. The whitening (zero at 3.5 Hz, pole at 35 Hz) is implemented in the main high-power photodiode used for controlling the differential arm-length in lock, while the dewhitening stage is built in the high voltage path between the high voltage amplifires and the electro-static drives. The relative coupling of all noise sources between these two points are reduced by a factor of 10 over the detection band.

3.2. Signal recycling loop

The signal recycling longitudinal loop is another feedback control system that introduces noise which couples to the gravitational wave channel. The noise in this feedback loop is dominated by shot noise in the sensing path. As a first attempt we lowered the bandwidth of this loop to get less noise in the detection band. This solution was sufficient for the time of S4, but of course there are limits for lowering the unity gain frequency which is currently about 20 Hz. Thus alternative approaches were needed to reduce the feedback noise to reach the design sensitivity of GEO 600.

Further improvement was gained by redesigning the corresponding loop filters aiming for a steeper lowpassing above unity gain. To achieve this we used manually optimised low pass IIR filters (implemented using a dSPACE system [7]) with 6 poles and 6 zeros, once the full lock of the dual recycled Michelson interferometer is established.

The next step is to subtract the noise introduced by the signal recycling loop from the gravitational wave signal by using the transfer function from signal recycling feedback point to *h(t)* [5].

[2] The application of feedback signals without using the square-root circuit inherently causes nonlinear noise effects. These are reduced by the fact that the small feedback signals are accompanied by a large bias voltage, and do not limit the detector sensitivity.

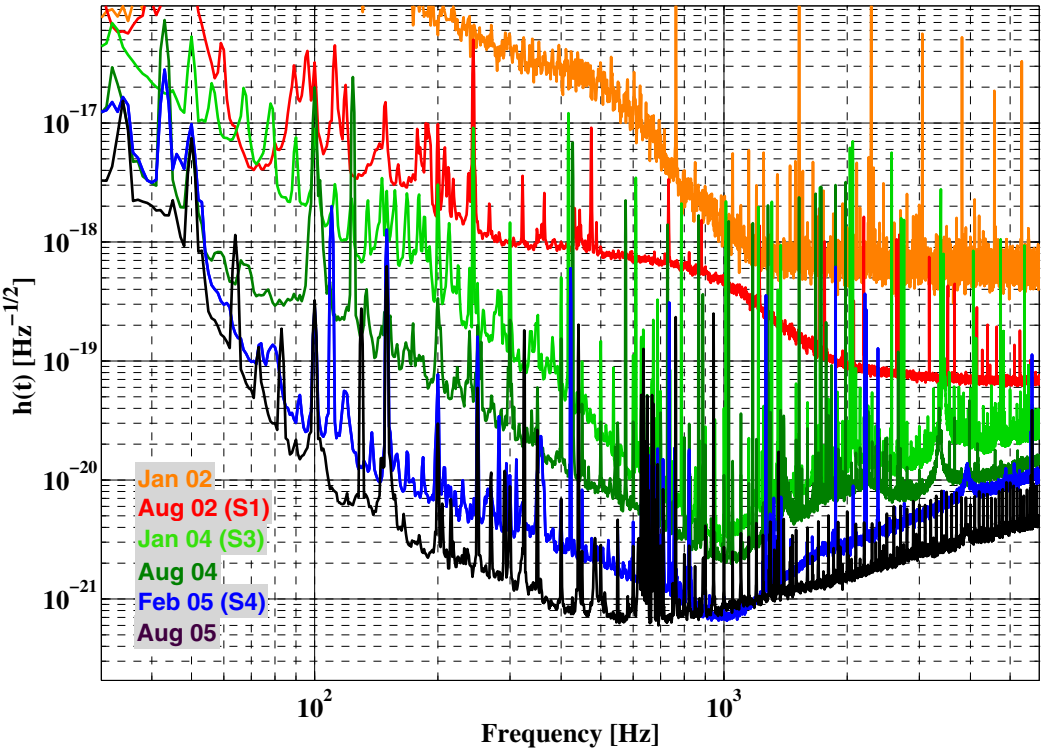

Figure 3. Sensitivity improvement of GEO 600 over the last three years.

Figure 3 shows the sensitivity improvement of GEO600 over the last three years.

4. Detector characterisation

4.1. Lock loss investigations

In the run-up to S4 we dedicated much effort to analysis of the origin of losses of lock and to elimination of their causes by improving the subsystem responsible. We developed a very simple method for investigating lock losses that is based on analysing time series of various detector signals, for example, errorpoints and feedbacks for longitudinal and alignment control, as well as physical environmental monitors. For each analysed signal, a standard level X_{nom} was defined which corresponds to a stably working system. In a second step an upper signal level, X_{max}, was set that determines the level where the corresponding subsystem stops working properly. For example, this can happen when a feedback signal gets to a level where the actuator is saturated. For analysing a lock loss we looked at all meaningful signals and found out which loop first left its operating point X_{nom} and crossed X_{max}. Afterwards it was then possible to go back in the chain and search for the disturbance that caused the subsystem to leave its operation point. Such a disturbance could be, for instance, an earthquake that causes a saturation in Michelson longitudinal feedback. With this method we investigated every lock loss during the S4 science run. Table 1 shows the results of this investigation.

4.2. Data quality

At the beginning of S4 we were in the unfortunate situation that strong excess noise was present for hour-long periods, while most of the time the detector was behaving reliably. After nine days

Reason for the loss of lock	**quantity**
Tractor passing one of the end stations	35
Glitches in the laser power stabilisation	25
Operator maintenance	22
2.5 Hz oscillation in Michelson alignment control	16
Stormy weather	14
Earthquakes	5
12 Hz oscillation in Michelson longitudinal control (MLC)	5
Coupled ringing in signal recycling alignment and MLC	3
Modecleaner 1 oscillation at 30 Hz	2
Horse galloping along the north building	2
End of range	1
Unclear	4
Total	**134**

Table 1. Causes for losses of lock during the LSC S4 science run.

we figured out that the excess noise was caused by transients on the Schnupp modulation used for the Michelson control, introduced by a fault in the resonant circuit going to the corresponding electro-optic modulator. We were able to eliminate the transients on the Schnupp modulation, thus the excess noise was removed (see [8] for further details).

The periods during which this excess noise was present are of little use for astrophysical searches. Consequently we needed to define a proper data quality indicator to flag these noisy times. In the end, it turned out that the χ^2 value originally developed as a quality indicator for the *h(t)* calibration process, can serve as a reasonable data quality flag.

4.2.1. χ^2 data quality flag For calibration of GEO 600 we use an on-line, time-domain calibration method which is described in detail in [9], [10] and [11]. Every second the optical transfer function of the detector is estimated by measuring amplitude and phase d_f at the frequencies f, where calibration lines are injected. Starting from this, an optimized model detector response m is calculated by an iterative procedure. The success of this modelling is measured by the χ^2 value:

$$\chi^2 = \sum_f \frac{(d_f - m_f)^2}{\sigma_f^2}, \tag{1}$$

where m_f is the best model at the calibration line frequencies and σ_f represents the noise floor around the calibration lines.

Figure 4 shows an example of the usefulness of the χ^2 data quality flag. The upper figure is a full time frequency plot of burst events, derived from the HACRmon pipeline [12]. In the center plot the corresponding time series of the peak sensitivity (RMS strain between 989 and 999 Hz) is shown. The bottom subplot contains the χ^2 value for the same time stretch. During the first three hours no excess noise was present, the peak sensitivity was nearly constant at a level of about $8 \times 10^{-22}/\sqrt{\text{Hz}}$ and the burst rate was low. Most of the following five hours are spoiled by the noise coming from the Schnupp modulation transients. Nevertheless, there are short time stretches for example around hour six with high data quality. We set a χ^2 threshold of 5000, above which the data are not going to be used. This threshold guarantees that times of poor data quality are taken out, while potential gravitational wave signals of low SNR are still available for gravitational wave searches.

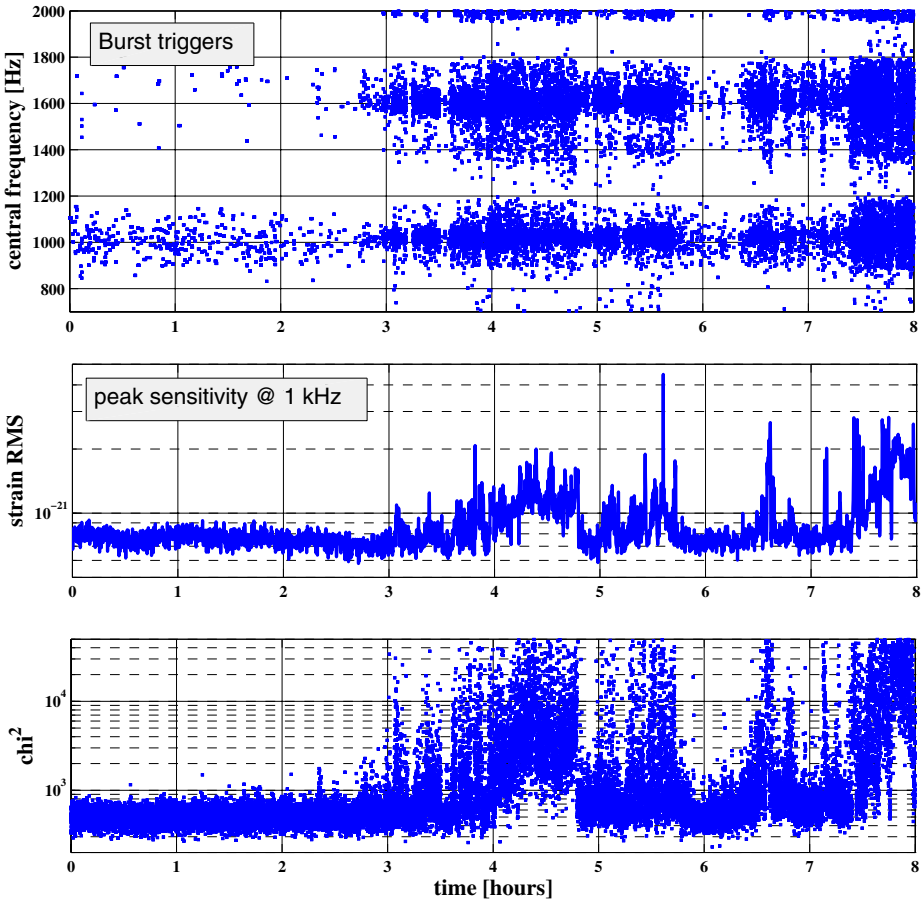

Figure 4. Transients on the Schnupp modulation spoil data quality.

4.3. Duty cycle during S4

During the 30 days of S4 the locking performance of GEO was impressive. The instrumental duty cycle of GEO 600 during S4 was greater than 96 % and for 95% of S4 we took science data. Many lock stretches were reasonably long, thus by only taking into account lock stretches longer than 10 hours, a duty cycle of larger than 70% is achieved. The longest lock was more than 52 hours.

Figure 5 shows the duty cycle of GEO 600 for various χ^2 cuts for three different minimum data stretches. [3]

5. Conclusion

GEO 600 is the first large scale gravitational-wave detector that uses the advanced optical technique of dual recycling. The detector commissioning done at GEO 600 resulted in an impressively stable detector behavior during the S4 LSC science run. A deeper understanding of the complex signal recycled interferometer was gained by intensive detector characterization work done over the last year.

[3] 300 seconds is the minimum time that will be used for burst analysis, while the inspiral analysis will only use lock stretches longer than 2048 seconds.

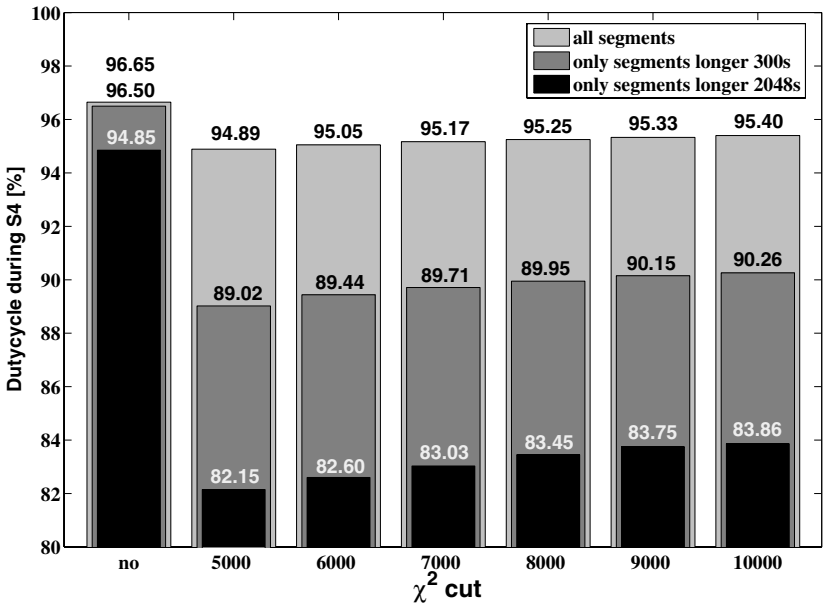

Figure 5. Duty cycle of GEO 600 during S4 for different χ^2-cuts.

Acknowledgments

The authors are grateful for support from PPARC and the University of Glasgow in the UK, and the BMBF and the state of Lower Saxony in Germany.

References

[1] Sigg D *et al* 2004 Commissioning of LIGO detectors *Class. Quantum Grav.* **21** S409-15.
[2] Acemese F *et al* 2004 Status of VIRGO *Class. Quantum Grav.* **21** S385-94.
[3] Takahaschi R (the TAMA Collaboration) 2004 Status of TAMA300 *Class. Quantum Grav.* **21** S403-8.
[4] Willke B *et al* 2004 Status of GEO 600 *Class. Quantum Grav.* **21** S417-23.
[5] Smith J R *et al* 2005 Projection of Technical Noise for Interferometric Gravitational-Wave Detectors, submitted to *Class. Quantum Grav.*
[6] Grote H, Making it Work: Second Generation Interferometry in GEO 600 !, PhD thesis, Hannover 2003
[7] http://www.dspaceinc.com/
[8] Lück H *et al* 2005 *Class. Quantum Grav.* this issue
[9] Hewitson M *et al* 2004 Principles of calibrating the dual-recycled GEO600 *Rev. Sci. Instrum.* **75**, 4702
[10] Hewitson M *et al* 2004 Calibration of the dual-recycled GEO 600 detector for the S3 science run *Class. Quantum Grav.* **21** No 20 S1711-S1722.
[11] Hewitson M *et al* 2005 Optimal time-domain combination of the two calibrated output quadratures of GEO 600, submitted to *Class. Quantum Grav.*
[12] Balasubramanian R *et al* 2005 Results from the first burst hardware injections performed on GEO 600 *Class. Quantum Grav.* **22** S3015-28.